Inorganic Chemistry

Article

pubs.acs.org/IC

Highly Luminescent and Thermally Stable Lanthanide Coordination Polymers Designed from 4-(Dipyridin-2-yl)aminobenzoate: Efficient Energy Transfer from Tb^{3+} to Eu^{3+} in a Mixed Lanthanide Coordination Compound

A. R. Ramya,[†] Debajit Sharma,[‡] Srinivasan Natarajan,[‡] and M. L. P. Reddy*[,†]

[†]Chemical Sciences and Technology Division, CSIR - Network of Institutes for Solar Energy, National Institute for Interdisciplinary Science and Technology (NIIST), Council of Scientific and Industrial Research (CSIR), Thiruvananthapuram 695 019, India

[‡]Framework Solids Laboratory, Solid State and Structural Chemistry Unit, Indian Institute of Science, Bangalore 560 012, India

Supporting Information

ABSTRACT: Herein, a new aromatic carboxylate ligand, namely, 4-(dipyridin-2-yl)aminobenzoic acid (HL), has been designed and employed for the construction of a series of lanthanide complexes (Eu^{3+} = **1**, Tb^{3+} = **2**, and Gd^{3+} = **3**). Complexes of **1** and **2** were structurally authenticated by single-crystal X-ray diffraction and were found to exist as infinite 1D coordination polymers with the general formulas $\{[Eu(L)_3(H_2O)_2]\}_n$ (**1**) and $\{[Tb(L)_3(H_2O)].(H_2O)\}_n$ (**2**). Both compounds crystallize in monoclinic space group *C*2/*c*. The photophysical properties demonstrated that the developed 4-(dipyridin-2-yl)aminobenzoate ligand is well suited for the sensitization of Tb^{3+} emission ($\Phi_{overall}$ = 64%) thanks to the favorable position of the triplet state ($^3\pi\pi^*$) of the ligand [the energy difference between the triplet state of the ligand and the excited state of Tb^{3+} (ΔE) = $^3\pi\pi^* - {}^5D_4$ = 3197 cm^{-1}], as investigated in the Gd^{3+} complex. On the other hand, the corresponding Eu^{3+} complex shows weak luminescence efficiency ($\Phi_{overall}$ = 7%) due to poor matching of the triplet state of the ligand with that of the emissive excited states of the metal ion ($\Delta E = {}^3\pi\pi^* - {}^5D_0$ = 6447 cm^{-1}). Furthermore, in the present work, a mixed lanthanide system featuring Eu^{3+} and Tb^{3+} ions with the general formula $\{[Eu_{0.5}Tb_{0.5}(L)_3(H_2O)_2]\}_n$ (**4**) was also synthesized, and the luminescent properties were evaluated and compared with those of the analogous single-lanthanide-ion systems (**1** and **2**). The lifetime measurements for **4** strongly support the premise that efficient energy transfer occurs between Tb^{3+} and Eu^{3+} in a mixed lanthanide system (η = 86%).

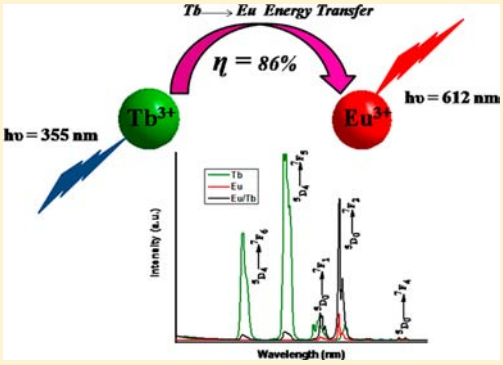

1. INTRODUCTION

Carboxylate ligands are highly complementary toward lanthanide metal ions because of the oxophilic nature of the latter.[1] Accordingly, lanthanide benzoates and their derivatives are stable and have attracted considerable attention for their potential use in a wide variety of fields because of their novel luminescent and magnetic properties.[2] In particular, when modified with light-harvesting moieties, benzoates have proven to be efficient sensitizers for lanthanide ions.[2a,3] In our recent work, it was demonstrated that replacement of the hydrogen atoms of the NH_2 moiety of *p*-aminobenzoic acid by benzyl groups had a significant influence on the distribution of the π-electron density within the ligand system and resulted in the development of a novel solid-state photosensitizer for Tb^{3+} with an overall quantum yield of 82%.[4] Subsequent investigations from our group also revealed that the presence of electron-releasing or -withdrawing groups on position 3 of the 4-benzyloxybenzoic acid ligand has a profound effect on the π-electron density of the ligands and consequently on the photosensitization of Ln^{3+} ions. Specifically, the presence of a methoxy substituent in this position results in a significant improvement in the photoluminescence (PL) efficiency of the terbium($^{3+}$) 3-methoxy-4-benzyloxybenzoate complex in comparison with that of the 4-benzyloxybenzoate complex (10–33%). By contrast, the introduction of a nitro group in the 3 position dramatically diminishes the PL efficiency of the terbium($^{3+}$) 3-nitro-4-benzyloxybenzoate complex because of the presence of a channel that permits dissipation of the excitation energy via the π^*-n transition of the nitro group in conjunction with the intraligand charge-transfer (ILCT) band.[5] Our latest communication disclosed that the replacement of high-energy C–H vibrations with fluorinated phenyl groups in 3,5-bis(benzyloxy)benzoate effectively improves the luminescence intensity and lifetimes of lanthanide complexes.[6] Inspired by the efficient sensitization of various lanthanide benzoates, herein, we have synthesized a new ligand, namely, 4-(dipyridin-2-yl)aminobenzoic acid, and utilized it for support of a series of new lanthanide coordination polymers featuring Eu^{3+}, Gd^{3+}, and Tb^{3+} cations. The designed 4-(dipyridin-2-yl)-

Received: March 29, 2012
Published: August 3, 2012

   dx.doi.org/10.1021/ic300654e | *Inorg. Chem.* 2012, 51, 8818–8826

aminobenzoate complexes of lanthanides were structurally characterized by single-crystal X-ray diffraction. The luminescent properties of the designed lanthanide benzoates have been systematically investigated and correlated with the triplet energy level of the newly developed benzoate molecule.

Energy-transfer processes involving two lanthanide ions in heterodinuclear complexes have been widely studied because they are proving useful in the design of miniature laser devices.[7] Remarkable enhancements and quenching of the photoluminescent emissions have been found recently in various mixed lanthanide carboxylate polymers.[7a,8] Cahill and coworkers reported terbium sensitization of europium in heterolanthanide coordination polymers.[9] The tunable emission of a widely varied family of lanthanide coordination polymers based on lanthanide terephthalate has been investigated, and it is proposed that Tb^{3+} can assist sensitization of Eu^{3+}.[10] Exploration of PL from polymer solid solutions has just started to emerge. Herein, we report energy transfer from 4-(dipyridin-2-yl)aminobenzoate-sensitized Tb^{3+} to Eu^{3+} in coordination polymers.

2. EXPERIMENTAL SECTION

Materials and Instrumentation. Europium(III) nitrate hexahydrate (99.9%), terbium(III) nitrate hexahydrate (99.9%), and gadolinium(III) nitrate hexahydrate (99.9%) were procured from Triebacher. Methyl 4-aminobenzoate (98%) and 2-bromopyridine (99.9%) were purchased from Sigma-Aldrich and used without further purification. All of the other chemicals used were of analytical reagent grade.

The C, H, and N elemental analyses were performed on a Perkin-Elmer series 2 elemental analyzer 2400. The IR spectra were recorded as KBr pellets on a Perkin-Elmer Spectrum One FT-IR spectrometer operating between 4500 and 400 cm^{-1}. A Bruker 500 MHz NMR spectrometer was used to record the ^1H NMR (500 MHz) and ^{13}C NMR (125.7 MHz) spectra of the new compound in a chloroform-*d* solution. The chemical shifts are reported in parts per million relative to tetramethylsilane ($SiMe_4$) for ^1H and ^{13}C NMR spectra. The mass spectra were recorded on a JEOL JSM 600 fast atom bombardment (FAB) high-resolution mass spectrometer (FAB-MS), and thermogravimetric analyses (TGA) were performed on a TG/DTA-6200 instrument (SII Nano Technology Inc., Japan) in a nitrogen atmosphere. Powder X-ray diffraction (XRD) patterns were recorded in the 2θ range of 10−70° using Cu Kα radiation (Philips X′pert). The quantitative microanalysis of the mixed lanthanide complex was carried out on an energy-dispersive spectrometer (Technai G^2 30LaB_6, ST with EDAX). UV−vis absorption spectra were recorded with a Shimadzu UV-2450 UV−vis spectrophotometer. All spectra were corrected for the background spectrum of the solvent. The absorbances of the ligand and complexes were measured in a CH_3CN/water mixture. PL spectra were recorded on a SPEX Fluorolog FL22 spectrofluorometer (HORIBA Jobin Yvon) equipped with a double-grating 0.22 m SPEX 1680 monochromator and a 450 W xenon lamp as the excitation source operating in the front-face mode. The lifetime and phosphorescence measurements were carried out at room temperature using a SPEX 1040 D phosphorimeter. The overall quantum yields for complexes **1** and **2** were determined under ligand excitation (355 nm) and are based on the absolute method using a calibrated integrating sphere in a SPEX Fluorolog spectrofluorometer as described elsewhere.[11,12] Each sample was measured several times under slightly different experimental conditions. The estimated error for the quantum yields is ±10%.[13]

The single-crystal XRD data were collected with a Bruker AXS Smart Apex CCD diffractometer at 293 K. The X-ray generator was operated at 50 kV and 35 mA using Mo Kα (λ = 0.71073 Å) radiation. The data were reduced using *SAINT*+,[14] and an empirical absorption correction was applied using the *SADABS* program.[15] The structure was solved and refined by using *SHELXL-97* in the *WINGX* suit of programs (v.1.63.04a).[16] All of the hydrogen positions were initially located in the difference Fourier maps, and for the final refinement, the hydrogen atoms were placed in geometrically ideal positions and refined in the riding mode. Final refinement included the atomic positions of all of the atoms, anisotropic thermal parameters for all of the non-hydrogen atoms, and isotropic thermal parameters for all of the hydrogen atoms. Full-matrix least-squares refinement against F^2 was carried out using the *WINGX* package of programs.[17] Selected crystal data and data collection and refinement parameters are listed in Table 1.

Table 1. Crystallographic and Refinement Data for 1 and 2

	1	2
formula	$C_{51}H_{40}N_9O_8Eu$	$C_{51}H_{36}N_9O_9Tb$
fw	1058.88	1077.81
cryst syst	monoclinic	monoclinic
space group	*C*2/*c*	*C*2/*c*
cryst size (mm^3)	0.12 × 0.04 × 0.03	0.12 × 0.03 × 0.02
temp (K)	296	293
a (Å)	30.2598(9)	29.502(3)
b (Å)	14.9444(4)	15.9006(10)
c (Å)	10.2439(3)	10.0813(8)
α (deg)	90	90
β (deg)	102.862(1)	102.716(9)
γ (deg)	90	90
V ($Å^3$)	4516.2(2)	4613.2(6)
Z	4	4
D_{calcd} (g cm^{-1})	1.557	1.552
μ(Mo Kα) (mm^{-1})	1.457	1.602
F(000)	2144.0	2168.0
R1 [$I > 2\sigma(I)$]	0.0178	0.0770
wR2 [$I > 2\sigma(I)$]	0.0448	0.1547
R1 (all data)	0.0226	0.1070
wR2 (all data)	0.0475	0.1691
GOF	1.039	0.974

Synthesis of Methyl 4-(Dipyridin-2-yl)aminobenzoate. The ester methyl 4-(dipyridin-2-yl)aminobenzoate was synthesized by a modified procedure reported elsewhere.[18] Potassium carbonate (1 g), potassium iodide (0.1 g), $CuSO_4 \cdot 5H_2O$ (0.1 g), and phenanthroline (0.1 g) were added to a solution of methyl 4-aminobenzoate (1 g, 6.6 mmol) in toluene (50 mL) followed by the addition of 2-bromopyridine (1.25 mL, 13.03 mmol). The resulting reaction mixture was refluxed for 24 h at 150 °C, and the solvents were evaporated to dryness. The residue was then dissolved in dichloromethane and washed with water. The resulting aqueous layer was further extracted with dichloromethane, and the combined organic extracts were dried with sodium sulfate, filtered, and evaporated at reduced pressure. The resulting residue obtained was purified by silica gel column chromatography using hexane/ethyl acetate, thereby affording the desired product as an off-white solid. Yield: 0.8 g (42%). ^1H NMR (500 MHz, $CDCl_3$): δ 8.29 (m, 2H, Ar−H), 7.92 (d, 2H, *J* = 8.5 Hz, Ar−H), 7.54 (m, 2H, Ar−H), 7.10 (d, 2H, *J* = 9 Hz, Ar−H), 6.94 (m, 4H, Ar−H), 3.83 (s, 3H, $-OCH_3$). ^{13}C NMR (125 MHz, $CDCl_3$): δ 165.56, 156.65, 148.31, 147.86, 136.92, 129.95, 124.80, 123.90, 118.20, 116.92, 50.96. FAB-MS: *m*/*z* 306.61 [$(M + 1)^+$]. FT-IR (KBr): ν_{max} 1715 (ν_{as}(C═O)), 1587, 1465 (ν_s(C═O)), 1430, 1289, 1172, 1106, 769, 703, 522 cm^{-1}.

Synthesis of 4-(Dipyridin-2-yl)aminobenzoic Acid (HL). Methyl 4-(dipyridin-2-yl)aminobenzoate (0.8 g, 2.62 mmol) was refluxed for 24 h in a 50 mL methanolic solution of NaOH (0.63 g, 5.75 mmol). The reaction mixture was poured into ice cold water and acidified with dilute HCl, and the resulting precipitate was filtered, washed, dried, and recrystallized from dichloromethane. Yield: 0.6 g (77%). ^1H NMR (500 MHz, $CDCl_3$): δ 8.40 (m, 2H, Ar−H), 7.93 (d, 2H, *J* = 8.5 Hz, Ar−H), 7.64 (m, 2H, Ar−H), 7.17 (d, 2H, *J* = 8.5 Hz,

dx.doi.org/10.1021/ic300654e | *Inorg. Chem.* 2012, 51, 8818−8826

Scheme 1. Synthesis of Ligand HL

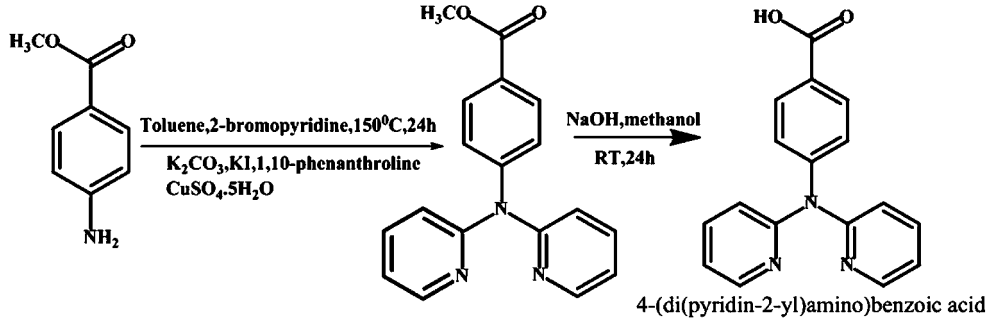

Ar−H), 7.05 (m, 4H, Ar−H). ^{13}C NMR (125 MHz, $CDCl_3$): δ 169.52, 157.49, 149.24, 148.69, 138.21, 131.60, 126.23, 125.28, 119.33, 118.07 (Figure S1 in the Supporting Information, SI). FAB-MS: m/z 292.59 [$(M + 1)^+$]. Elem anal. Calcd (found) for $C_{17}H_{13}O_2N_3$ (291.31): C, 70.09 (70.05) ; H, 4.50 (4.31); N, 14.42 (14.22). FT-IR (KBr): ν_{max} 1699 (ν_{as}(C═O)), 1598, 1466, 1434 (ν_s(C═O)), 1286, 1172, 1009, 770, 741, 520 cm^{-1}.

Syntheses of Lanthanide Complexes. All metal complexes were prepared in a similar manner in air by mixing stoichiometric amounts of ligand (1.5 mmol) and $Ln(NO_3)_3{\cdot}6H_2O$ (0.5 mmol; Ln = Eu, Tb, or Gd) in ethanol in the presence of NaOH (1.5 mmol). Precipitation took place immediately, and the reaction mixture was stirred subsequently for 12 h at room temperature. The crude product was filtered, washed with ethanol. and dried. The resulting complexes were then purified by recrystallization from a dichloromethane/methanol solvent mixture. Single crystals of the terbium and europium complexes suitable for single-crystal X-ray study were obtained from an ethanol/water solvent mixture after storage for 4 weeks at room temperature.

$[Eu(L)_3(H_2O)_2](H_2O)$ (1). Elem anal. Calcd (found) for $C_{51}H_{42}N_9O_9Eu$ (1076.91): C, 56.88 (56.66); H, 3.93 (3.66); N, 11.70 (11.45). FT-IR (KBr): ν_{max} 3402 (ν(O−H)), 1643 (ν_{as}(C═O)), 1594 (ν_{as}(C═O)), 1469, 1426 (ν_s(C═O)), 1400 (ν_s(C═O)), 1321, 1274, 1154, 773 cm^{-1}. FAB-MS: m/z 1022.22 {$[Eu(L)_3]^+$; Figure S2 in the SI}.

$[Tb(L)_3(H_2O)](H_2O)$ (2). Elem anal. Calcd (found) for $C_{51}H_{40}N_9O_8Tb$ (1065.86): C, 57.46 (57.33); H, 3.78 (3.81); N, 11.82 (11.60). FT-IR (KBr): ν_{max} 3391 (ν(O−H)), 1643 (ν_{as}(C═O)), 1594 (ν_{as}(C═O)), 1469, 1424 (ν_s(C═O)), 1404 (ν_s(C═O)), 1321, 1274, 1154, 773 cm^{-1}. FAB-MS: m/z 1046.64 {$[Tb(L)_3{\cdot}(H_2O)]^+$; Figure S2 in the SI}.

$[Gd(L)_3(H_2O)_2]$ (3). Elem anal. Calcd (found) for $C_{51}H_{40}N_9O_8Gd$ (1063.75): C, 57.57 (57.45); H, 3.79 (3.81); N, 11.85 (11.74). FT-IR (KBr): ν_{max} 3409 (ν(O−H)), 1643 (ν_{as}(C═O)), 1594 (ν_{as}(C═O)), 1468, 1428 (ν_s(C═O)), 1402 (ν_s(C═O)), 1294, 1153, 774 cm^{-1}. FAB-MS: m/z 1046.83 {$[Gd(L)_3{\cdot}(H_2O) + 1]^+$; Figure S2 in the SI}.

$[Eu_{0.5}Tb_{0.5}(L)_3(H_2O)_2]$ (4). Elem anal. Calcd (found) for $C_{51}H_{40}N_9O_8$ $Eu_{0.5}Tb_{0.5}$ (1062.38): C, 57.66 (57.49); H, 3.79 (3.57); N, 11.86 (12.00). FT-IR (KBr): ν_{max} 3401 (ν(O−H)), 1646 (ν_{as}(C═O)), 1595 (ν_{as}(C═O)), 1469, 1428 (ν_s(C═O)), 1405 (ν_s(C═O)), 1320, 1274, 1153, 854, 773 cm^{-1}. FAB-MS: m/z 1041.36 {$[Eu(L)_3{\cdot}(H_2O) + 1]^+$}, 1028.85 {$[Tb(L)_3]^+$; Figure S2 in the SI}. The 1:1 molar ratios of Tb^{3+}/Eu^{3+} in a mixed Ln^{3+} complex were further confirmed by energy-dispersive spectrometry (EDS) analysis (Eu/Tb = 1.02).

3. RESULTS AND DISCUSSION

The ligand HL was synthesized (yield: 77%) in two steps starting from commercially available 4-aminobenzoate, as outlined in Scheme 1. The newly designed ligand was identified on the basis of ^{1}H and ^{13}C NMR spectroscopy (Figure S1 in the SI), FAB-MS, FT-IR, and elemental analysis. The protocols used for the syntheses of lanthanide 4-(dipyridin-2-yl)-aminobenzoate complexes are summarized in the Experimental Section. The elemental analysis data of the complexes revealed that in each case the Ln^{3+} ion had reacted with the corresponding benzoate ligand in a metal-to-ligand mole ratio of 1:3. The FT-IR spectrum of the ligand evidenced intense absorption bands characteristic of the carboxylate groups at 1434 and 1699 cm^{-1}, which are assigned to the symmetric ν_s(C═O) and asymmetric ν_{as}(C═O) vibrations, respectively. These bands in the spectrum of the free ligand, which are assigned to the stretching vibrations of the nonionized carboxylic group, are shifted in the FT-IR spectra of **1**−**4**, thus confirming that the ligand is completely ionized and, hence, in accordance with the single-crystal X-ray structures. Moreover, the symmetric and asymmetric stretching vibrational modes of the carboxylate groups in complexes **1**−**4** are further split into two peaks (Table S1 in the SI). The differences between the asymmetric and symmetric stretching vibrational modes ($\Delta\nu_{(C=O)} = \nu_{as} - \nu_s$) fall in the ranges 215−219 and 190−194 cm^{-1}, which indicates that carboxylate groups are coordinated to Ln^{3+} ions in bidentate bridging and chelating modes.[19] The broad band observed at 3400 cm^{-1} for complexes **1**−**4** is attributed to the characteristic ν_{OH} stretching vibration and is indicative of the presence of water molecules. The 1:1 molar ratios of Tb^{3+}/Eu^{3+} in a mixed Ln^{3+} complex **4** were further confirmed by EDS analysis (Eu/Tb = 1.02; Figure S3 and Table S2 in the SI). The powder XRD patterns of complexes **1**−**4** are similar to each other, thus implying that these complexes are isostructural (Figure S4 in the SI).

Thermal Properties. The thermal stabilities of complexes **1**, **2**, and **4** were examined by TGA in the 30−1000 °C range, and the corresponding thermograms are depicted in Figure S5 in the SI. It is interesting to note that compounds **1** and **2** are thermally stable up to ∼450 °C, with a first weight loss between 90 and 200 °C in complex **1** (found, 4.70%; calcd, 5.01%), corresponding to the release of one uncoordinated and two coordinated water molecules. On the other hand, the loss of two water molecules was noted in the case of complex **2** (found, 3.40%; calcd, 3.38%) due to the elimination of one lattice and one coordinated water molecules. It can be noted from the thermogram of complex **4** that it is stable up to ∼430 °C, with a first weight loss (found, 3.30%; calcd, 3.39%), which accounts for the elimination of two coordinated water molecules. The second weight loss, between 450 and 850 °C for complex **1** (found, 79.80%; calcd, 80.87%), is attributed to thermal decomposition of three ligand molecules. On the other hand, in the case of complex **2**, the second weight loss noted between 450 and 770 °C (found, 81.90%; calcd, 81.71%) and the loss occurring between 450 and 850 °C (found, 81.20%; calcd, 81.98%) in complex **4** can also be due to the loss of three ligand moieties. The total weight losses are compatible with

dx.doi.org/10.1021/ic300654e | Inorg. Chem. 2012, 51, 8818−8826

formulas, and the masses of the final products correspond to the complete combustion of the complexes to their corresponding metal oxides (Eu_2O_3 or Tb_4O_7). The differences observed in TGA of complexes **1** and **2** are essentially due to the different hydration states of the Ln^{3+} cations and also can be attributed to lanthanide contraction.[20]

X-ray Crystal Structures. Single-crystal XRD studies reveal the 1D coordination polymeric nature of both **1** and **2** (Figures 1 and 2). However, these complexes have different coordination environments. The pertinent data collection parameters and a listing of significant bond distances and angles for both compounds are depicted in Tables 1 and 2, respectively. Compounds **1** and **2** crystallize in the monoclinic space group *C*2/*c*. The lanthanide centers in compounds **1** and **2** are doubly bridged by carboxylate groups of the 4-(dipyridin-2-yl)-aminobenzoate ligands and thereby form infinite 1D chains.

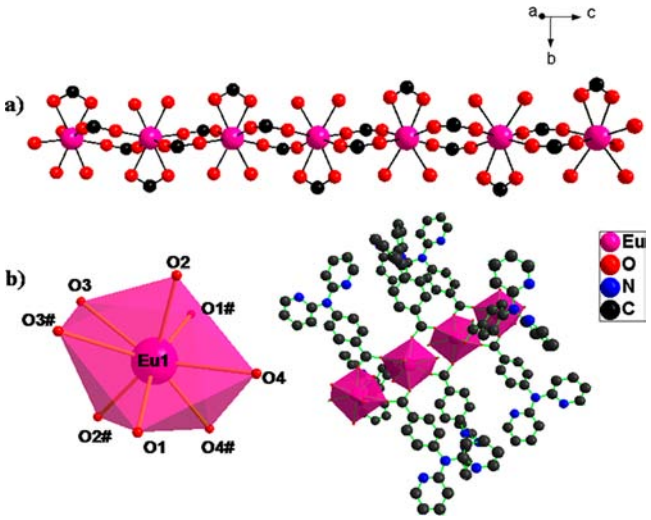

Figure 1. (a) 1D coordination polymer chain of complex **1**. (b) Coordination environment of complex **1**. All hydrogen atoms are omitted for clarity. Symmetry codes: A, $1 - x, y, 1.5 - z$; B, $1 - x, 2 - y, 2 - z$; C, $1 - x, 2 - y, 1 - z$; D, x, y, z.

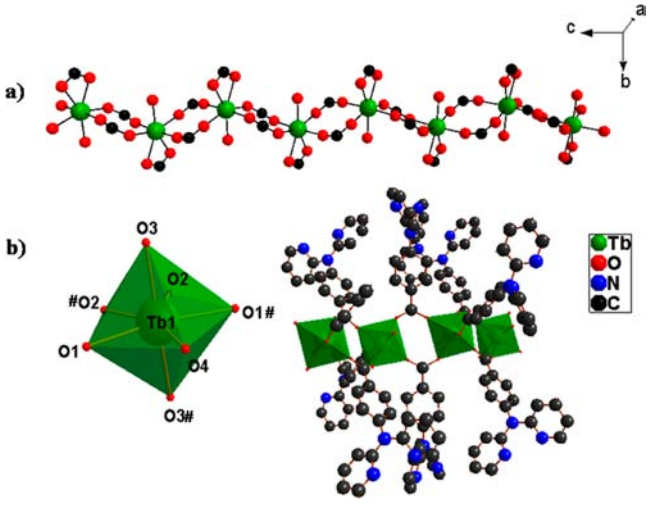

Figure 2. (a) 1D wavelike coordination polymer chain of complex **2**. (b) Coordination environment of complex **2**. All hydrogen atoms are omitted for clarity. Symmetry codes: A, $x, 2 - y, -{}^1/_2 + z$; B, $-x, 2 - y, 1 - z$; C, $-x, y, {}^1/_2 - z$; D, x, y, z.

Table 2. Selected Bond Lengths (Å) and Angles (deg) for 1 and 2

1		2	
Eu1−Eu1	5.122	Tb1−Tb1	5.278
Eu1−O1	2.312(2)	Tb1−O1	2.240(2)
Eu1−O2	2.330(2)	Tb1−O2	2.428(2)
Eu1−O3	2.514(2)	Tb1−O3	2.325(2)
Eu1−O4	2.539(2)	Tb1−O4	2.349(2)
Eu1−O1#	2.312(2)	Tb1−O1#	2.240(2)
Eu1−O2#	2.330(2)	Tb1−O2#	2.428(2)
Eu1−O3#	2.514(2)	Tb1−O3#	2.325(2)
Eu1−O4#	2.539(2)		
O1−Eu1−O1	153.60(7)	O2−Tb1−O2	53.69(2)
O1−Eu1−O2	82.59(5)	O1−Tb1−O3	91.55(2)
O1−Eu1−O2	101.23(5)	O3−Tb1−O3	156.2(2)
O2−Eu1−O2	163.42(7)	O1−Tb1−O4	87.94(12)
O1−Eu1−O3	74.45(5)	O3−Tb1−O4	78.10(12)
O1−Eu1−O3	81.79(5)	O1−Tb1−O2	91.3(2)
O2−Eu1−O3	73.68(4)	O3−Tb1−O2	75.05(17)
O3−Eu1−O3	51.79(6)	O3−Tb1−O2	128.74(16)
O1−Eu1−O4	134.22(5)	O2−Tb1−O4	153.15(11)
O4−Eu1−O4	68.77(6)		

It is interesting to note that compound **2** forms a 1D wavelike strand; on the other hand, compound **1** forms a straight chain. This may be due to the differences in their coordination environments. The Eu1 center of **1** is coordinated to four carboxylate oxygen atoms of the bridging 4-(dipyridin-2-yl)aminobenzoate ligands, two carboxylate oxygen atoms of the chelating 4-(dipyridin-2-yl)aminobenzoate ligand, and two water molecules. The coordination geometry around the Eu1 center can be described as a distorted square antiprism, with O−Eu1−O bond angles ranging from 51.79° to 163.42°. In contrast to the Eu1 center in **1**, the Tb1 center of **2** is surrounded by seven oxygen atoms in a distorted pentagonal-bipyramidal arrangement, with O−Tb1−O bond angles ranging from 53.69° to 156.2°. The Tb1 center in **2** is coordinated to four carboxylate oxygen atoms from the bridging benzoate ligands, two carboxylate oxygen atoms from the chelating benzoate ligand, and one oxygen atom from the water molecule.

The longest Ln1−O bonds involve the oxygen atoms of the bidentate chelating ligands [Eu1−O3, 2.514 Å; Eu1−O3#, 2.514 Å; Tb−O2, 2.428 Å; Tb−O2#, 2.428 Å], and the shortest bonds are associated with bridging carboxylate ligands [Eu−O1, 2.312 Å; Eu−O2, 2.330 Å, Eu−O1#, 2.312 Å; Eu−O2#, 2.330 Å; Tb−O1, 2.240 Å; Tb−O1#, 2.240 Å, Tb−O3, 2.325 Å; Tb−O3#, 2.325 Å]. These trends in the distances are found to be same as those observed in lanthanide carboxylate complexes featuring bidentate chelating and bridging modes.[1a,21] The carboxylate bridges also adopt a syn−anti confirmation in both **1** and **2** to exhibit Ln1−Ln1 distances of 5.122 Å in **1** and 5.278 Å in **2**. The distance between adjacent terbium centers is found to be larger than the Eu1−Eu1 distance. This can be attributed to the differences in their coordination environments in view of the presence of two inner-sphere water molecules in complex **1**, while complex **2** has only one. The most noteworthy structural features of these compounds are the presence of free Lewis basic pyridyl sites within the 1D coordination polymer, which may have a potential utility of these compounds for the recognition and sensing of metal ions.

dx.doi.org/10.1021/ic300654e | *Inorg. Chem.* 2012, 51, 8818−8826

Electronic Spectra of the Ln^{3+} Complexes. The absorption spectra of the free ligand and corresponding Ln^{3+} complexes (**1**−**4**) have been recorded in the CH_3CN/water mixture (CH_3CN, 60%; water, 40%; $c = 2 \times 10^{-5}$ M) at 298 K and are depicted in Figure 3. The ligand displays an absorption

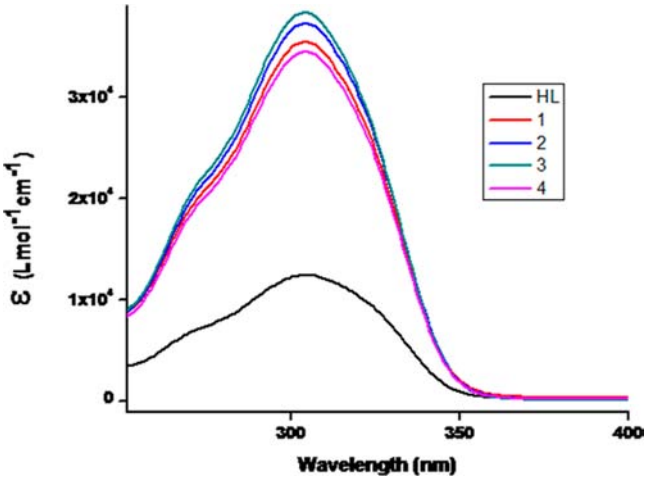

Figure 3. UV−vis absorption spectra of the ligand HL and complexes **1**−**4** in CH_3CN/water mixture (CH_3CN, 60%; water, 40%; $c = 2 \times 10^{-5}$ M).

band localized in the UV region with a molar absorption coefficient (ε_{max}) of 1.2×10^4 L mol^{-1} cm^{-1} (λ_{max} = 305 nm) that is classically observed for $\pi\pi^*$ transitions of benzoic acid ligands. The trends in the absorption spectra of the complexes are identical with those observed for the free ligand. The molar absorption coefficients of **1**−**4** are found to be 3.5×10^4, 3.7×10^4, 3.8×10^4, and 3.4×10^4 L mol^{-1} cm^{-1}, respectively, showing the strong ability of the complexes to absorb light in the 250−350 nm region, with maxima at 305 nm. The absorption coefficients for the complexes are about 3 times higher compared that to the free ligand, in line with the formation of 3:1 (ligand/metal) complexes. These features point to the ligand being an adequate light-harvesting chromophore for the sensitization of lanthanide luminescence.

Photophysical Properties. In the present study, the gadolinium(3+) 4-(dipyridin-2-yl)aminobenzoate complex (**3**) has been utilized to probe the triplet energy level of the newly developed sensitizer 4-(dipyridin-2-yl)aminobenzoate to assess its efficiency in the energy-transfer process to the lanthanides. It is widely recognized that Gd^{3+} complexes are a popular choice for elucidating triplet energy levels of the ligand for the following reasons: (1) Because of its heavy atom effect, the Gd^{3+} ion increases the rate of intersystem crossing. (2) The first excited-state electronic levels of Gd^{3+} are at high energies (^5I_J at around 36900 cm^{-1}), there is no gadolinium emission in the visible range, and all luminescence observed is due to the ligand part of the complex. Thus, radiative decay from a triplet excited state becomes the predominant energy migration pathway. Compound **3** exhibits ligand phosphorescence as a broad band centered at 435 nm after excitation at 305 nm at 77 K (Figure S6 in the SI). The triplet energy level ($^3\pi\pi^*$) of the ligand was estimated by reference to its lower-wavelength emission edge (422 nm; 23697 cm^{-1}) of the low-temperature phosphorescence spectrum of the Gd^{3+} complex **3**. It can be noted that the triplet energy level of the ligand is found to be higher than that of the emitting levels of both $^5D_4$ of Tb^{3+} or $^5D_0$ of Eu^{3+}, thus indicating that the designed ligand can act as an antenna for photosensitization of these Ln^{3+} ions.[22] To elucidate the energy migration pathways in Ln^{3+} complexes, it was also necessary to determine the singlet energy level ($^1\pi\pi^*$) of the ligand. The singlet ($^1\pi\pi^*$) energy level of this ligand was determined by reference to the UV−vis upper absorption edge of the Gd^{3+} complex **3** (Figure 3), and the value was found to be 346 nm (28900 cm^{-1}). It is well documented that an efficient ligand-to-metal energy transfer requires a good intersystem-crossing efficiency, which is maximized when the energy difference between singlet and triplet states, $\Delta E(^1\pi\pi^* - ^3\pi\pi^*)$, is close to 5000 cm^{-1}.[23] Thus, in the present study, it amounts to 5203 cm^{-1}, and therefore the newly developed ligand has a good intersystem-crossing efficiency.

The excitation spectrum of the Eu^{3+} complex **1** (in the solid state) at room temperature, monitored around the peak of the intense $^5D_0 \rightarrow {}^7F_2$ transition consists of a broad band and several narrow bands (Figure 4). The broad band peaking at

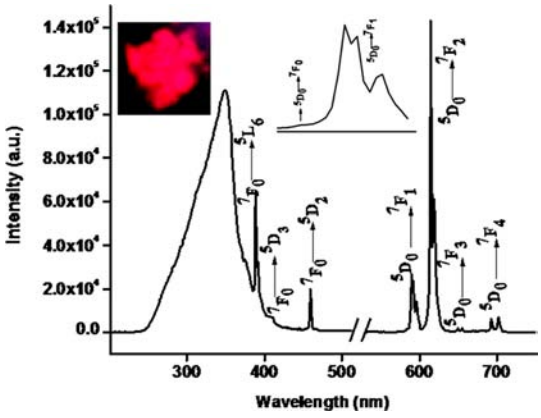

Figure 4. Room-temperature excitation and emission spectra for complex **1** (λ_{ex} = 355 nm) with emission monitored at approximately 612 nm.

355 nm is attributed to the $\pi\pi^*$ ligand transition, and the narrow bands are assigned to transitions of the Eu^{3+} intra-$^4F_6$ ion, from $^7F_0$ to $^5L_6$ (394 nm), $^5D_3$ (414 nm), and $^5D_2$ (464 nm) levels.[24] However, these transitions are weaker than the absorption of the organic ligand and are overlapped by a broad excitation band, which proves that luminescence sensitization via excitation of the ligand is much more efficient than the direct excitation of the Eu^{3+} ion absorption level. The emission spectrum of **1** was recorded under the maximum excitation wavelength at 355 nm. The emission spectrum is composed of the first excited state, $^5D_0$, and the ground septet, ^7F_J (J = 0−4) of Eu^{3+}.[25] The transition $^5D_0 \rightarrow {}^7F_0$ is very weak and is situated at 582 nm. The moderately strong transition $^5D_0 \rightarrow {}^7F_1$ splits into three peaks at 589, 592, and 596 nm. The hypersensitive transition $^5D_0 \rightarrow {}^7F_2$ consists of a strong band at 614 nm, resulting in red luminescence. The peaks at about 650 and 656 nm correspond to the characteristic $^5D_0 \rightarrow {}^7F_3$ transition. It is also noted that four splitting peaks of the $^5D_0 \rightarrow {}^7F_4$ transition occurs at 693, 697, 701, and 705 nm.

The steady-state excitation and emission spectra of the Tb^{3+} complex **2** at room temperature are depicted in Figure 5. The excitation spectrum of **2** monitored around the peak of the intense $^5D_4 \rightarrow {}^7F_5$ transition of the Tb^{3+} ion displays a broad band between the 250 and 400 nm range with a maximum at approximately 355 nm, which can be assigned to the $^1\pi\pi^*$

dx.doi.org/10.1021/ic300654e | Inorg. Chem. 2012, 51, 8818−8826

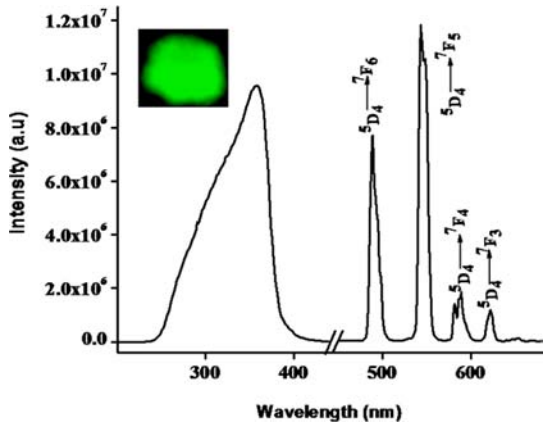

Figure 5. Room-temperature excitation and emission spectra for complex **2** (λ_{ex} = 355 nm) with emission monitored at approximately 545 nm.

transition of the antenna molecule. The absence of any absorption bands due to the f−f transitions of the Tb^{3+} cation proves that luminescence sensitization via excitation of the ligand is more sensitive than the direct excitation of the Tb^{3+} ion. The room-temperature emission spectrum of the Tb^{3+} complex exhibits the characteristic emission bands of Tb^{3+} (λ_{ex} = 355 nm) centered at 490, 545, 585, and 620 nm, which result from deactivation of the $^5D_4$ excited state to the corresponding ground state ^7F_J (J = 6, 5, 4, 3) of the Tb^{3+} ion.[2c,5,26] The more intense transition centered at 545 nm corresponds to the transition of $^5D_4 \rightarrow {}^7F_5$. Moreover, the ligand-centered emission is not detected, thus implying the existence of an efficient ligand-to-metal energy-transfer process in this complex.

The excited state $^5D_0$ (Eu^{3+}) and $^5D_4$ (Tb^{3+}) lifetime values (τ_{obs}) were measured at both ambient (298 K) and low temperatures (77 K) for the Ln^{3+} complexes **1** and **2**, by monitoring within the more intense lines of the $^5D_0 \rightarrow {}^7F_2$ and $^5D_4 \rightarrow {}^7F_5$ transitions, respectively (Figures S7−S9 in the SI), and the pertinent values are summarized in Table 3. The observed luminescent decay profiles correspond to single-exponential functions, thus implying the presence of only one emissive Ln^{3+} center. The shorter $^5D_0$ lifetime (τ_{obs} = 428 ± 2 μs) noted for the Eu^{3+} complex **1** at 298 K may be due to the dominant nonradiative decay channels associated with vibronic coupling because of the presence of two water molecules in the coordination sphere of this complex.[27] This value is essentially temperature-dependent, with τ_{obs} (759 ± 7 μs) approximately doubled upon going from 298 to 77 K, thereby reflecting the presence of thermally activated deactivation processes. This effect has been well documented for many hydrated europium carboxylate complexes.[4,5] A longer $^5D_4$ lifetime value at 298 K (938 ± 7 μs) has been observed for the Tb^{3+} complex even when the solvent molecules are present in the first coordination sphere because they are well-known to be vibrational deactivators of the excited states of the Ln^{3+} ions.[28] The energy gap between the luminescent and ground state manifolds are approximately 12000 and 14800 cm^{-1} for Eu^{3+} and Tb^{3+}, respectively. Relatively efficient coupling of the Eu^{3+} excited states occurs for the third vibrational overtone of the proximate O−H oscillators ($\nu_{OH} \sim 3300-3500\ cm^{-1}$) and for the fourth harmonic in the case of Tb^{3+}, which is consistent with the less efficient quenching observed in the case of Tb^{3+}, where the Franck−Condon overlap factor is less favorable.[29] The $^5D_4$ lifetime value of the Tb^{3+} complex is found to be essentially temperature-independent, with τ_{RAD} (970 ± 7 μs) varying by ∼3% upon going from 298 to 77 K, thereby reflecting the absence of thermally activated deactivation processes.

In order to understand the photophysical properties of the designed ligand, it was appropriate to analyze the luminescent behavior in terms of eq 1,[30] where $\Phi_{overall}$ and Φ_{Ln} represent the ligand-sensitized and intrinsic luminescent quantum yields of Ln^{3+}. Φ_{sen} represents the efficiency of the ligand-to-metal energy transfer:

$$\Phi_{overall} = \Phi_{sen}\Phi_{Ln} \quad (1)$$

Here, Φ_{Ln} can be calculated from the following equation:

$$\Phi_{Ln} = \left(\frac{A_{RAD}}{A_{RAD} + A_{NR}}\right) = \frac{\tau_{obs}}{\tau_{RAD}} \quad (2)$$

The intrinsic quantum yield of Eu^{3+} could not be determined experimentally upon direct f−f excitation because of its very low absorption intensity. Therefore, the radiative lifetime of Eu^{3+} can be calculated from eq 3,[31] where n represents the refractive index of the medium. An average index of refraction equal to 1.5 was employed in the calculation.[32] $A_{MD,0}$ (14.65 s^{-1}) represents the spontaneous emission probability of the $^5D_0 \rightarrow {}^7F_1$ transition in vacuo, and I_{TOT}/I_{MD} signifies the ratio of the total integrated intensity of the corrected Eu^{3+} emission spectrum to the integrated intensity of the magnetic-dipole $^5D_0 \rightarrow {}^7F_1$ transition.

$$A_{RAD} = \frac{1}{\tau_{RAD}} = A_{MD,0}n^3\left(\frac{I_{TOT}}{I_{MD}}\right) \quad (3)$$

The intrinsic quantum yield for Tb^{3+} (Φ_{Tb}) was estimated using eq 4 with the assumption that the decay process at 77 K in a deuterated solvent is purely radiative.[33]

$$\Phi_{Tb} = \tau_{obs(298K)}/\tau_{obs(77K)} \quad (4)$$

Table 3 summarizes the $\Phi_{overall}$, Φ_{Ln}, Φ_{sen}, and radiative (A_{RAD}) and nonradiative (A_{NR}) decay rates. Solid-state measurements gave a quantum yield of 64% for the terbium(3+) 4-(dipyridin-2-yl)aminobenzoate complex **2**. Conversely, the corresponding Eu^{3+} complex **1** shows poor luminescent efficiency with low quantum yield (7%). A poor sensitization efficiency for the Eu^{3+} complex **1** has been noted for the newly constructed benzoate ligand mainly because of the larger energy gap between the

Table 3. Radiative (A_{RAD}) and Nonradiative (A_{NR}) Decay Rates, $^5D_0/^5D_4$ Lifetimes (τ_{obs}), Radiative Lifetimes (τ_{RAD}), Intrinsic Quantum Yields (Φ_{Ln}), Energy-Transfer Efficiencies (Φ_{sen}), and Overall Quantum Yields ($\Phi_{overall}$) for Complexes 1 and 2

complex	A_{RAD} (s^{-1})	A_{NR} (s^{-1})	τ_{obs} (μs)	τ_{RAD} (μs)	Φ_{Ln} (%)	Φ_{sen} (%)	$\Phi_{overall}$ (%)
1	282	2071	428 ± 2 759 ± 7[a]	3540	12	58	7 ± 0.7
2			938 ± 7	970 ± 7	97	66	64 ± 6

[a]77 K.

dx.doi.org/10.1021/ic300654e | Inorg. Chem. 2012, 51, 8818−8826

triplet state and the $^5D_0$ level of Eu^{3+} $\Delta E(^3\pi\pi^*-^5D_0)$ = 6447 cm^{-1} for **1**. Therefore, a lower quantum yield has been observed in the Eu^{3+} complex. On the other hand, complex **2** exhibits a higher quantum yield ($\Phi_{overall}$ = 64%) and an efficient ligand-to-metal energy transfer (Φ_{sen} = 66%) because of the superior match of the triplet energy level of HL to that of the Tb^{3+} emitting level [$\Delta E(^3\pi\pi^*-^5D_4)$ = 3197 cm^{-1}].

Energy Transfer from Tb^{3+} to Eu^{3+} in a Mixed Lanthanide Complex. The PL emission spectrum of compound **4** is compiled in Figure 6 along with the emission

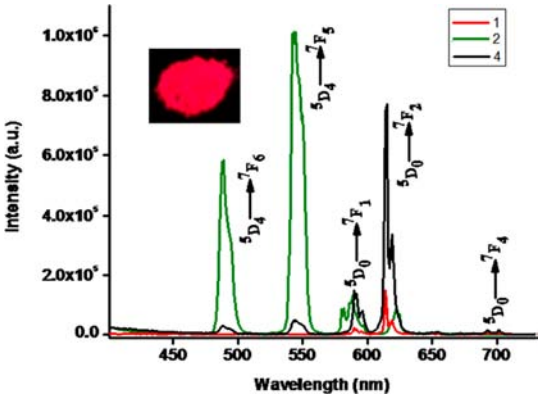

Figure 6. Room-temperature emission spectra for complexes **1**, **2**, and **4**, excited at 355 nm.

spectrum of coordination polymers of complexes **1** and **2**. The mixed lanthanide complex exhibits an enhanced luminescent intensity at 614 nm (5.48-fold) corresponding to the $^5D_0 \rightarrow {}^7F_2$ transition of the Eu^{3+} ion compared to the isostructural Eu^{3+} complex **1** because of the presence of the Tb^{3+} ion in complex **4**. On the other hand, a considerable decrease in the luminescent intensity at 545 nm (22.7-fold) corresponding to the $^5D_4 \rightarrow {}^7F_5$ transition compared to the isostructural Tb^{3+} complex **2**, indicating the highest efficiency of Tb^{3+} to Eu^{3+} energy transfer. Furthermore, the color in the luminescent image of the mixed Ln^{3+} complex shows bright-red emission under UV light.

The lifetime measurements of the Ln^{3+} emissions in mixed-lanthanide systems represent an important tool for the demonstration of energy transfer between the Ln^{3+} ions.[7,34] Lifetime values for the excited-state energy levels for complex **4** were determined from their respective luminescent decay profiles at room temperature (Figure S10 in the SI). The lifetimes of Tb^{3+} and Eu^{3+} emissions in a mixed-Ln^{3+} system provides further evidence that energy transfer from the Tb^{3+} to Eu^{3+} centers is indeed occurring because the lifetime of the Tb^{3+} emission decreases by approximately 86% (down to 132 ± 1 μs from 938 ± 7 μs in **2**). In contrast, the lifetime of the Eu^{3+} emission increases moderately to 525 ± 1 μs (from 428 ± 2 μs in **1**). This can be explained as being due to a decrease of the concentration quenching by dilution of the Eu^{3+} ions. The energy-transfer efficiency (η) for the purely dipole−dipole, through-space energy-transfer mechanism can be quantified by eqs 5 and 6:[34e]

$$\eta = 1 - (\tau/\tau_0) \quad (5)$$

$$\eta = 1/[1 + (R/R_0)^6] \quad (6)$$

where τ and τ_0 are the lifetimes of luminescence of the donor in the presence and absence of the acceptor, R_0 is the distance required for 50% energy transfer, and R is the actual distance between the donor and acceptor. The energy-transfer efficiency estimated as per eq 5 was found to be 86% when τ = 132 ± 1 μs and τ_0 = 938 ± 7 μs. On the other hand, as per eq 6, the energy-transfer efficiency of η = 96% was obtained when it has been assumed that R = 5.2 Å and R_0 = 9.0 Å (the value for R_0 usually lies between 8 and 10 Å for Eu^{3+}/Tb^{3+} pairs in helicates[34a]). This efficiency is approximately similar to the value calculated experimentally for the mixed complex **4** system based on lifetime values. It is therefore a strong possibility that intrachain energy transfer occurs predominantly via a dipole−dipole mechanism. The efficiency of energy transfer observed in the present system is comparable to that of heterometallic lanthanide helicates developed by Piguet and co-workers, which display superior energy-transfer yields of 72% and 82%.[34a]

In addition to the above-mentioned Ln → Ln energy-transfer pathways, it is well demonstrated that the general mechanism for the sensitization of Ln^{3+} ion luminescence via the "antenna effect" involves the following steps: (i) UV absorption by the organic chromophore, which results in excitation to the first excited-state singlet (S_1); (ii) intersystem crossing from the singlet to the triplet state (T_1); (iii) intermolecular energy transfer from the ligand-centered triplet state to the excited 4f states of the Ln^{3+} ions; (iv) radiative transition from the Ln^{3+} ion emissive states to lower energy states, which results in the characteristic Ln^{3+} emission.[35] Thus, the intramolecular energy migration efficiency from the organic chromophore ligand to the central Ln^{3+} ion is one of the key factors that influences the luminescent properties of these Ln^{3+} complexes. Taking the mixed Ln^{3+} complex **4** as a typical example, the schematic diagram representing energy-transfer pathways is summarized in Figure 7.

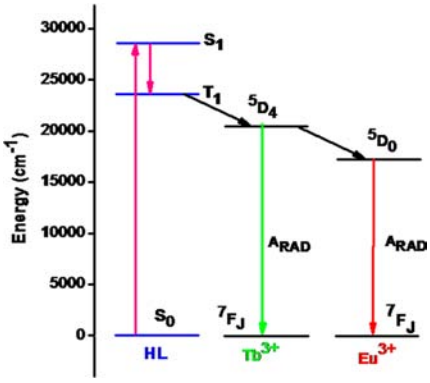

Figure 7. Schematic representation of the energy-transfer mechanism for complex **4**.

4. CONCLUSIONS

In summary, we have demonstrated the design, synthesis, and characterization of a new class of highly luminescent thermally stable lanthanide coordination polymers that utilizes a novel HL ligand to indirectly excite the lanthanide metal center. The terbium coordination polymers show high quantum yields ($\Phi_{overall}$ = 64 ± 6%) and long lifetimes (τ_{obs} = 938 ± 7 μs), supporting the hypothesis that the superior match of the triplet state of the ligand with that of the $^5D_4$ excited-state level of the metal ion. In contrast to the foregoing, the Eu^{3+} coordination polymer features a weak luminescence efficiency ($\Phi_{overall}$ = 7 ± 0.7%) due to poor matching of the triplet state of the ligand

dx.doi.org/10.1021/ic300654e | Inorg. Chem. 2012, 51, 8818−8826

with the emissive excited states of the metal ion. Another noteworthy feature from the current study is an efficient Tb^{3+}-to-Eu^{3+} energy transferability in a heteronuclear lanthanide complex, and hence it is a potential candidate for applications in the field of color displays, luminescence sensors, and structural probes.

■ ASSOCIATED CONTENT

Supporting Information

X-ray crystallographic data of complexes **1** and **2** in CIF format, ^{1}H and ^{13}C NMR spectra for ligand HL, FAB-MS for complexes **1**−**4**, EDS analysis results, XRD patterns, TGA data, phosphorescence spectrum of the gadolinium complex **3** at 77 K, luminescence decay profiles, and IR vibrational frequencies. This material is available free of charge via the Internet at http://pubs.acs.org.

■ AUTHOR INFORMATION

Corresponding Author

*E-mail: mlpreddy55@gmail.com.

Notes

The authors declare no competing financial interest.

■ ACKNOWLEDGMENTS

The authors acknowledge financial support from the CSIR, New Delhi, India (CSIR-TAPSUN project, SSL, NWP-55). A.R.R. thanks CSIR for the award of a Junior Research Fellowship.

■ REFERENCES

(1) (a) Deacon, G. B.; Hein, S.; Junk, P. C.; Justel, T.; Lee, W.; Turner, D. R. *Cryst. Eng. Comm.* **2007**, *9*, 1110−1123. (b) Busskamp, H.; Deacon, G. B.; Hilder, M.; Junk, P. C.; Kynast, U. H.; Lee, W. W.; Turner, D. R. *Cryst. Eng. Comm.* **2007**, *9*, 394−411. (c) Hilder, M.; Junk, P. C.; Kynast, U. H.; Lezhnina., M. M. *J. Photochem. Photobiol. A* **2009**, *202*, 10−20.

(2) (a) Li, Y.; Zheng, F. K.; Liu, X.; Zou, W. Q.; Guo, G. C.; Lu, C. Z.; Huang, J. S. *Inorg. Chem.* **2006**, *45*, 6308−6316. (b) Lam, A. W.-H.; Wong, W.-T.; Gao, S.; Wen, G.; Zhang, X.-X. *Eur. J. Inorg. Chem.* **2003**, 149−163. (c) Lucky, M. V.; Sivakumar, S.; Reddy, M. L. P.; Paul, A. K.; Natarajan, S. *Cryst. Growth Des.* **2011**, *11*, 857−864.

(3) (a) Li, X.; Zhang, Z.-Y.; Zou, Y. Q. *Eur. J. Inorg. Chem.* **2005**, *14*, 2909−2918. (b) Viswanathan, S.; de Bettencourt-Dias, A. *Inorg. Chem.* **2006**, *45*, 10138−10146.

(4) Ramya, A. R.; Reddy, M. L. P.; Cowley, A. H.; Vasudevan, K. V. *Inorg. Chem.* **2010**, *49*, 2407−2415.

(5) Sivakumar, S.; Reddy, M. L. P.; Cowley, A. H.; Vasudevan, K. V. *Dalton Trans.* **2010**, *39*, 776−786.

(6) Sivakumar, S.; Reddy, M. L. P. *J. Mater. Chem.* **2012**, *22*, 10852−10859.

(7) (a) Froidevaux, P.; Bünzli, J.-C. G. *J. Phys. Chem.* **1994**, *98*, 532−536. (b) Bettinelli, M.; Flint, C. D. *J. Phys.: Condens. Matter* **1990**, *2*, 8417. (c) Kellendonk, F.; Blasse, G. *J. Chem. Phys.* **1981**, *75*, 561. (d) Biju, S.; Reddy, M. L. P.; Jayasankar, C. K.; Cowley, A. H.; Findlater, M. *J. Mater. Chem.* **2009**, *19*, 1425−1432. (e) Kim Anh, T.; Strek, W. *J. Lumin.* **1988**, *42*, 205.

(8) (a) Choi, C. L.; Yen, Y. F.; Sung, H. H.-Y.; Siu, A. W.-H.; Jayarathne, S. T.; Wong, K. S.; Williams, I. D. *J. Mater. Chem.* **2011**, *21*, 8547−8549. (b) Comby, S.; Scopelliti, R.; Imbert, D.; Charbonniere, L.; Ziessel, R. F.; Bünzli, J.-C. G. *Inorg. Chem.* **2006**, *45*, 3158−3160. (c) Guo, H.; Zhu, Y.; Qiu, S.; Lercher, J. A.; Zhang, H. *Adv. Mater.* **2010**, *22*, 4190−4192.

(9) de Lill, D. T.; de Bettencourt-Dias, A.; Cahill, C. L. *Inorg. Chem.* **2007**, *46*, 3960−3965.

(10) Kerbellec, N.; Kustaryono, D.; Haquin, V.; Etienne, M.; Diaguebonne, C.; Guillou, O. *Inorg. Chem.* **2009**, *48*, 2837−2843.

(11) (a) De Mello, C.; Wittmann, H. F.; Friend, R. H. *Adv. Mater.* **1997**, *9*, 230−232. (b) Pålsson, L.-O.; Monkman, A. P. *Adv. Mater.* **2002**, *14*, 757−758. (c) Shah, B. K.; Neckers, D. C.; Shi, J.; Forsythe, E. W.; Morton, D. *Chem. Mater.* **2006**, *18*, 603−608.

(12) (a) Colle, M.; Gmeiner, J.; Milius, W.; Hillebrecht, H.; Brütting, W. *Adv. Funct. Mater.* **2003**, *13*, 108−112. (b) Saleesh Kumar, N. S.; Varghese, S.; Rath, N. P.; Das, S. *J. Phys. Chem. C* **2008**, *112*, 8429−8437.

(13) Eliseeva, S. V.; Kotova, O. V.; Gumy, F.; Semenov, S. N.; Kessler, V. G.; Lepnev, L. S.; Bünzli, J.-C. G.; Kuzmina, N. P. *J. Phys. Chem. A* **2008**, *112*, 3614−3626.

(14) *SMART* (version 5.628), *SAINT* (version 6.45a), *XPREP*, *SHELXTL*; Bruker AXS Inc.: Madison, WI, 2004.

(15) Sheldrick, G. M. *Siemens Area Correction Absorption Correction Program*; University of Gottingen: Gottingen, Germany, 1994.

(16) Sheldrick, G. M. *SHELXL-97 Program for Crystal Structure Solution and Refinement*; University of Gottingen: Gottingen, Germany, 1997.

(17) Farrugia, J. L. *J. App. Crystallogr.* **1999**, *32*, 837−838.

(18) Kirin, S. I.; Yennawar, H. P.; Williams, M. E. *Eur. J. Inorg. Chem.* **2007**, *23*, 3686−3694.

(19) (a) Deacon, G. B.; Phillips, R. *J. Coord. Chem. Rev.* **1980**, *33*, 227−250. (b) Teotonio, E. E. S.; Brito, H. F.; Felinto, M. C. F. C.; Thompson, L. C.; Young, V. G.; Malta, O. L. *J. Mol. Struct.* **2005**, *751*, 85−94. (c) Raphael, S.; Reddy, M. L. P.; Cowley, A. H.; Findlater, M. *Eur. J. Inorg. Chem.* **2008**, *28*, 4387−4394.

(20) (a) Soares-Santos, P. C. R.; Cunha-Silva, L.; Almeida Paz, F. A.; Rute, A. S.; Ferreira, A.; Rocha, J.; Carlos, L. D.; Nogueira, H. I. S. *Inorg. Chem.* **2010**, *45*, 3428−3440. (b) Mahata, P.; Ramya, K. V.; Natarajan, S. *Chem.—Eur. J.* **2008**, *14*, 5839−5850.

(21) Liu, M.-S.; Yu, Q.-Y.; Cai, Y.-P.; Su, C.-Y.; Lin, X.-M.; Zhou, X.-X.; Cai, J.-W. *Cryst. Growth Des.* **2008**, *8*, 4083−4091.

(22) Latva, M.; Takalo, H.; Mukkala, V. M.; Matachescu, C.; Rodriguez-Ubis, J. C.; Kanakare, J. *J. Lumin.* **1997**, *75*, 149−169.

(23) Steemers, F. J.; Verboom, W.; Reinhoudt, D. N.; Vander Tol, E. B.; Verhoeven, J. W. *J. Am. Chem. Soc.* **1995**, *117*, 9408−9414.

(24) (a) Biju, S.; Ambili Raj, D. B.; Reddy, M. L. P.; Kariuki, B. M. *Inorg. Chem.* **2006**, *45*, 10651−10660. (b) Li, X.; Sun, H.-L.; Wu, X.-S.; Qiu, X.; Du, M. *Inorg. Chem.* **2010**, *49*, 1865−1871. (c) Wan, Y.-H.; Zheng, X.-J.; Wang, F.-Q.; Zhou, X.-Y.; Wang, K.-Z.; Jin, L.-P. *Cryst. Eng. Comm.* **2009**, *11*, 278−283.

(25) (a) Ambili Raj, D. B.; Francis, B.; Reddy, M. L. P.; Butorac, R. R.; Lynch, V. M.; Cowley, A. H. *Inorg. Chem.* **2010**, *49*, 9055−9063. (b) Divya, V.; Biju, S.; Luxmi Varma, R.; Reddy, M. L. P. *Dalton Trans.* **2010**, *20*, 5220−5227. (c) Francis, B.; Ambili Raj, D. B.; Reddy, M. L. P. *Dalton Trans.* **2010**, *39*, 8084−8092.

(26) (a) Remya, P. N.; Biju, S.; Reddy, M. L. P.; Cowley, A. H.; Findlater, M. *Inorg. Chem.* **2008**, *47*, 7396−7404. (b) Xia, J.; Zhao, B.; Wang, H.-S.; Shi, W.; Ma, Y.; Song, H.-B.; Cheng, P.; Liao, D.-Z.; Yan, S.-P. *Inorg. Chem.* **2007**, *46*, 3450−3458. (c) Dieke, G. H. *Spectra and Energy levels of Rare Earth Ions in Crystals*; Interscience: New York, 1968.

(27) (a) Ambili Raj, D. B.; Biju, S.; Reddy, M. L. P. *Inorg. Chem.* **2008**, *47*, 8091−8100. (b) Biju, S.; Reddy, M. L. P.; Cowley, A. H.; Vasudevan, K. V. *J. Mater. Chem.* **2009**, *19*, 5179−5187.

(28) (a) Samuel, A. P. S.; Moore, E. G.; Melchior, M.; Xu, J.; Raymond, K. N. *Inorg. Chem.* **2008**, *47*, 7535−7544. (b) Biju, S.; Reddy, M. L. P.; Cowley, A. H.; Vasudevan, K. V. *Cryst. Growth Des.* **2009**, *9*, 3562−3569. (c) Sivakumar, S.; Reddy, M. L. P.; Cowley, A. H.; Butorac, R. R. *Inorg. Chem.* **2011**, *50*, 4882−4891.

(29) (a) Dossing, A. *Eur. J. Inorg. Chem.* **2005**, *8*, 1425−1434. (b) Beeby, A.; Clarkson, I. M.; Dickins, R. S.; Faulkner, S.; Parker, D.; Royle, L.; de Sousa, A. S.; Williams, J. A. G.; Woods, M. *J. Chem. Soc., Perkin Trans. 2* **1999**, *3*, 493−503.

(30) (a) Xiao, M.; Selvin, P. R. *J. Am. Chem. Soc.* **2001**, *123*, 7067−7073. (b) Quici, S.; Cavazzini, M.; Marzanni, G.; Accorsi, G.; Armaroli, N.; Ventura, B.; Barigelletti, F. *Inorg. Chem.* **2005**, *44*, 529−537.

(c) Comby, S.; Imbert, D.; Anne-Sophie, C.; Bünzli, J.-C. G.; Charbonniere, L. J.; Ziessel, R. F. *Inorg. Chem.* **2004**, *43*, 7369−7379.
(31) (a) Shavaleev, N. M.; Eliseeva, S. V.; Scopelliti, R.; Bünzli, J.-C. G. *Inorg. Chem.* **2010**, *49*, 3927−3936. (b) Zucchi, G.; Olivier, M.; Pierre, T.; Gumy, F.; Bünzli, J.-C. G.; Michel, E. *Chem.—Eur. J.* **2009**, *15*, 9686−9696.
(32) Pavithran, R.; Saleesh Kumar, N. S.; Biju, S.; Reddy, M. L. P.; Alves, S., Jr.; Freire, R. O. *Inorg. Chem.* **2006**, *45*, 2184−2192.
(33) (a) Nasso, I.; Bedel, S.; Galaup, C.; Picard, C. *Eur. J. Inorg. Chem.* **2008**, *12*, 2064−2074. (b) Sabbatini, N.; Guardigli, M.; Lehn, J. M. *Coord. Chem. Rev.* **1993**, *123*, 201−228.
(34) (a) Piguet, C.; Bünzli, J.-C. G.; Bernardinelli, G.; Hopfgartner, G.; Williams, A. F. *J. Am. Chem. Soc.* **1993**, *115*, 8197. (b) Elhabiri, M.; Scopelliti, R.; Bünzli, J.-C. G.; Piguet, C. *J. Am. Chem. Soc.* **1999**, *121*, 10747−10762. (c) Ananias, D.; Kostova, M.; Almeida Paz, F. A.; Ferreira, A.; Carlos, L. D.; Klinowski, J.; Rocha, J. *J. Am. Chem. Soc.* **2004**, *126*, 10410. (d) Sendor, D.; Hilder, M.; Juestel, T.; Junk, P. C.; Kynast, U. H. *New J. Chem.* **2003**, *27*, 1070. (e) Lewis, D. J.; Glover, B. G.; Solomons, M. C.; Pikramenou, Z. *J. Am. Chem. Soc.* **2011**, *133*, 1033−1043.
(35) (a) Binnemans, K. *Chem. Rev.* **2009**, *109*, 4283−4374. (b) Bünzli, J.-C. G. *Chem. Rev.* **2010**, *110*, 2729−2755.